Valence-shell dependence of the pygmy dipole resonance: E1 strength difference in ^{50,54}Cr

P. C. Ries, H. Pai, T. Beck, J. Beller, M. Bhike, V. Derya, U. Gayer, J. Isaak, B. Löher, Krishichayan, L. Mertes, N. Pietralla, C. Romig, D. Savran, M. Schilling, W. Tornow, S. Typel, V. Werner, J. Wilhelmy, A. Zilges, and M. Zweidinger

Valence-shell dependence of the pygmy dipole resonance: E1 strength difference in ^{50,54}Cr

P. C. Ries,[1, *] H. Pai,[1, 2] T. Beck,[1] J. Beller,[1] M. Bhike,[3] V. Derya,[4] U. Gayer,[1] J. Isaak,[1, 5]
B. Löher,[1] Krishichayan,[3] L. Mertes,[1] N. Pietralla,[1] C. Romig,[1] D. Savran,[5] M. Schilling,[1]
W. Tornow,[3] S. Typel,[1, 5] V. Werner,[1] J. Wilhelmy,[4] A. Zilges,[4] and M. Zweidinger[1]

[1]*Institut für Kernphysik, Technische Universität Darmstadt, 64289 Darmstadt, Germany*
[2]*Saha Institute of Nuclear Physics, Kolkata 700064, India*
[3]*Triangle Universities Nuclear Laboratory, Duke University, Durham, NC 27708, U.S.A.*
[4]*University of Cologne, Institute for Nuclear Physics, 50937 Köln, Germany*
[5]*GSI Helmholtzzentrum für Schwerionenforschung, Planckstr. 1, 64291 Darmstadt, Germany*
(Dated: July 23, 2019)

Background: The low-lying electric dipole strength provides insights on the parameters of the nuclear equation of state via its connection with the pygmy dipole resonance and nuclear neutron skin thickness.

Purpose: Complement the systematic of the pygmy dipole resonance and first study its behavior across the $N = 28$ neutron shell closure.

Methods: Photon-scattering cross sections of states of ^{50,54}Cr were measured up to an excitation energy of 9.7 MeV via the nuclear resonance fluorescence method using γ-ray beams from bremsstrahlung and Compton backscattering.

Results: Transitions strengths, spin and parity quantum number and average branching ratios for 55 excited states, 44 of which were observed for the first time, were determined. The comparison between the total observed strengths of the isotopes ^{50,52,54}Cr shows a significant increase above the shell closure.

Conclusions: The evolution of the pygmy dipole resonance is heavily influenced by the shell structure.

With the recent observation of a merging binary neutron-star system via gravitational waves by the LIGO-Virgo collaboration, unforeseen new approaches in the field of astrophysics have been made possible. The simultaneous detection of corresponding electromagnetic radiation has been referred to as the beginning of the era of *multi-messenger* astronomy [1]. Thus, it has been shown that neutron-star mergers are the predominant sites for nucleosynthesis via the r-process [2]. Predictions for neutron-star mergers as well as other systems, like heavy-ion collisions or supernovae explosions, depend on a reliable description of the nuclear equation of state (EOS). Its crucial role is emphasized in current physics research [3–6]. As part of the EOS, the symmetry energy describes the variation of the energy per nucleon when the neutron-proton ratio changes. It is commonly expanded in a Taylor series around the saturation density of symmetric nuclear matter. The symmetry energy at saturation, $J = S_0$, and its density dependence, the slope parameter L, are the leading coefficients of the expansion as a function of isospin asymmetry and nuclear density, where L is most uncertain. Its determination is highly desired in order to allow for precise aforementioned predictions.

Thus, the investigation of the density dependence of the symmetry energy draws much attention of both theoretical and experimental research. The expansion parameters show a strong correlation with the neutron skin thickness of atomic nuclei [7]. In turn, the neutron skin thickness is related to the electric dipole response of nuclei, more precisely to the nuclear polarizability representing the inverse energy-weighted sum-rule of electric dipole excitation strength [8]. Recently, it has been measured for $^{[48]}$Ca [9]. The so-called pygmy dipole resonance (PDR) [10] is low lying in energy and consequently contributes appreciably to the nuclear polarizability due to the inverse energy-weighting of the $E1$-transition strength in the expression for the nuclear polarizability. A gradual increase of the PDR strength with neutron excess is expected if the PDR is interpreted as a collective dipole excitation, where collectivity is prevalently defined by a highly coherent wave function in the single-particle base. This leads to the following questions: How much of a collective mode is the PDR, especially at its onset in the mass $A \approx 50$ region? And what impact does the specific valence space for electric dipole excitations has on the evolution of strength associated with the PDR?

The electric dipole response has been studied over several decades and shows common features in many nuclei. As such, the isovector giant dipole resonance (GDR) was one of the first nuclear structure phenomena observed and described [11–14]. The excitation energy of this broad structure is around 10 to 20 MeV and the GDR is usually interpreted as an out-of-phase oscillation between all protons and all neutrons within the nucleus.

At the center of current attention is the pygmy dipole resonance [8, 15]. Originally referring to the accumulation of dipole transition strength near the neutron separation threshold [16], the distinction between the PDR and a low-energy tail of the GDR is difficult. The PDR

exhausts a few percent of the overall dipole strength, which is concentrated in the GDR. A separation may be achieved by experimental and theoretical considerations that are sensitive to the mixed isovector and isoscalar character of the PDR [17, 18]. A frequently used interpretation of the PDR is a collective oscillation of a saturated proton-neutron core against a neutron skin [19–21] in clear distinction to the GDR.

The nuclear resonance fluorescence method (NRF) is an appropriate experimental tool to investigate the PDR. It is selective to dipole-excited states, because of the real photons' preferred low angular momentum transfer [22]. An accumulation of electric dipole transition strength as a typical indication for the PDR has already been reported for many nuclei, most of them within the vicinity of a shell closure. Examples are the Mo [23–25] and Sn [26, 27] isotopic chains and the $N = 50$ isotonic chain ^{86}Kr [28], ^{88}Sr [29], ^{89}Y [30] and ^{90}Zr [31]. So far the lightest nuclei showing a PDR-like structure are the nickel isotopes [32, 33]. In contrast to that, very little transition strength was reported from NRF experiments with excitation energies up to 10 MeV on calcium isotopes [34, 35]. In order to fill the gap in this systematic between Ca and Ni, the stable even-even chromium isotopes were examined in this work. The results for ^{52}Cr have already been reported in Ref. [36–38]. In this publication, data for ^{50}Cr and ^{54}Cr are presented. In particular, this is the first time an evolution of the electric dipole strength across a neutron shell closure and the dependence of the PDR on the neutron valence space are investigated with the means of NRF. Considering the minuscule natural abundances of the neutron-deficient isotopes of the only other suitable candidates argon or cerium, chromium might very well be the only possible element for such a study in the foreseeable future.

A set of complementary NRF experiments were conducted at two major research facilities, one part at the Darmstadt High Intensity Photon Setup (DHIPS) [39] of the superconducting Darmstadt linear accelerator S-DALINAC at the Institut für Kernphysik Darmstadt [40] and the other part at the High-Intensity γ-ray Source facility HIγS of the Duke Free Electron Laser Laboratory at TUNL [41].

At DHIPS, the electron beam is stopped in a copper or gold radiator target. An aluminum beam attenuator is used to suppress background caused by low-energy photons of the emitted bremsstrahlung. These photons are then collimated by a copper collimator onto the photon scattering target. Parts of the photons are resonantly absorbed and the target nuclei are excited and subsequently decay directly to the ground state (elastic scattering) or via intermediate states (inelastic scattering). The emitted γ-rays are detected by three Compton-suppressed high-purity germanium (HPGe) detectors with detection efficiencies of 100% compared to a standard NaI detector at 1.33 MeV. The HPGe detectors are positioned at 90°, 95° and 130° with respect to the incident γ-beam. This allows to determine the spin quantum num-

ber of the states in even-even nuclei, since the ratio of the angular distributions differs the most for dipole and quadrupole transition at these angles. In addition the continuous bremsstrahlung spectra is utilized for a simultaneous measurements of the excited states' cross sections.

At HIγS, the γ-ray beams are produced via Compton backscattering of a free-electron laser (FEL). Collimation of the scattered photons then results in a quasi-monoenergetic photon beam with an energy width of roughly 3% , which is continuously tunable and retains the FEL polarization of nearly 100%. Up to four HPGe detectors were placed at the target position in a rectangular cross perpendicular to the beam. This arrangement allows for the determination of the parity quantum numbers of dipole-excited states from the polar asymmetry ϵ of emitted γ-rays [42]:

$$\epsilon = \frac{N_\parallel - N_\perp}{N_\parallel + N_\perp} = Q\Sigma P_\gamma \qquad (1)$$

Here $N_{\parallel,\perp}$ are the efficiency-corrected intensities in and perpendicular to the beams' polarization plane. The angular distribution of the emitted γ-rays with magnetic (electric) radiation character is maximum (minimal) in the polarization plane of the beam and minimal (maximum) perpendicular to it. The analyzing power Σ of $0^+ \to 1^\Pi \to 0^+$ cascades are either $\Sigma = +1$ or $\Sigma = -1$. The beam polarization P_γ is known to exceed 99% [43]. However, the absolute values for the asymmetries are attenuated due to the limited polarization sensitivity $Q \approx 90\%$ of our setup because of the finite solid angles of the detectors and the finite target size.

At DHIPS two measurements with bremsstrahlung endpoint energies 9.7 and 7.5 MeV were conducted for each examined nucleus. The spin quantum numbers are determined from DHIPS data through the azimuthal angular distributions. For spin sequences $0 \to 1 \to 0$ and $0 \to 2 \to 0$ the ratio $w_i = W_{0\to i\to 0}(90°)/W_{0\to i\to 0}(130°)$ is equal to $w_1 = 0.71$ and $w_2 = 2.26$, respectively. Spin quantum numbers were assigned accordingly through the efficiency-corrected peak areas extracted from the measurements at DHIPS. The assignments of both quantum numbers are usually rather unambiguous, but may complement each other in uncertain cases, due to the limited combinations emerging from excitation using NRF. The photon flux was determined from the known cross sections of excited states of ^{11}B , which was added to the target as an calibration standard, hence integrated cross section of the isotopes of intend were obtained relative to ^{11}B as described in Ref. [25]. Measurements at two different endpoint energies were performed in order to identify inelastic transitions to excited states. In this manner, 55 states have been observed in ^{50}Cr and ^{54}Cr, 44 of those for the first time. All findings are listed in the supplemental material [44]. See e.g. [45] for details. Fig. 1 shows spectra of ^{50}Cr and ^{54}Cr taken at a polar angle of $\theta = 130°$.
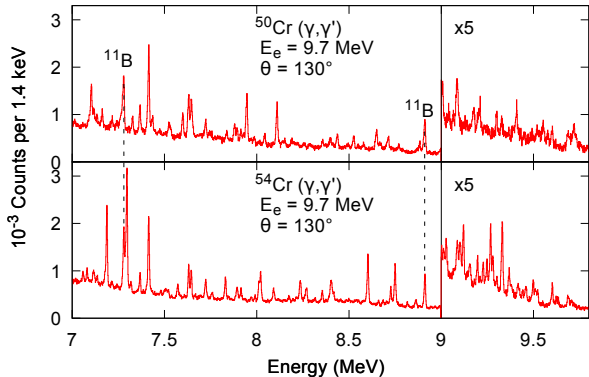
FIG. 1. Extract of the Compton-suppressed ^{50,54}Cr spectra at $130°$ scattering angle. These spectra are recorded at DHIPS via the NRF method utilizing bremsstrahlung from an electron beam with an energy of 9.7 MeV.

In order to obtain parity quantum numbers and further information on the energy dependence of the inelastic photon-scattering cross section, additional experiments were conducted at the γ^3-setup [46] at HIγS. The beam was tuned to various energy settings for a couple of hours each, which completely cover the energy range from 5.5 to 9.8 MeV. An example of spectra is given in Fig. 2, while parity assignments are shown in Fig. 3.
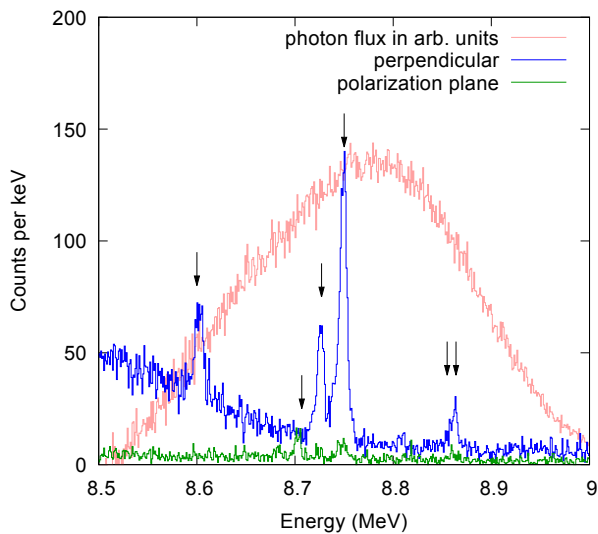

FIG. 2. Spectra recorded at the HIγS facility. The red (light gray) curve shows the incident quasi-monoenergetic photon flux of an energy setting at 8.8 MeV measured by a dedicated detector at $0°$. The green (gray) spectrum is recorded in the polarization plane of the incoming photon beam and the blue (dark gray) one perpendicular to that. The arrows mark observed transitions of ^{54}Cr. One can clearly assess a parity quantum number based on the difference in intensity for each transition between the green (gray) and blue (dark gray) spectrum.
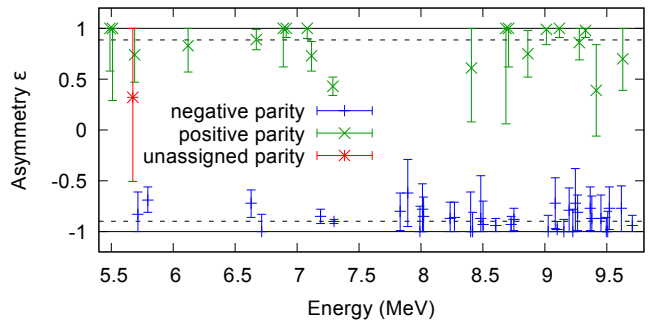

FIG. 3. Azimuthal intensity asymmetries derived from data taken at HIγS for the example of ^{54}Cr. The colors correspond to the assigned parity quantum numbers. The dashed lines show the weighted averages, +0.88 for positive and -0.90 for negative parity. These are indicators for the great sensitivity of this method in comparison to the ideal values of +1 and -1.

The individual settings of the monoenergetic beam at HIγS allow for the determination of an average branching ratio for each range of excitation energy. Considering the known angular distributions of photons emitted in a $0_1^+ \rightarrow 1_i^- \rightarrow 2_1^+ \rightarrow 0_1^+$ cascade, the average branching ratio b for each energy setting is determined via

$$b = \frac{N_0^-}{N_0^- + \frac{2N^-}{3}}. \tag{2}$$

Here, N_0^- is the sum of the efficiency-corrected intensities of all observed electric dipole transitions to the ground-state and $N^- = 2N_{2_1^+,\parallel} - N_{2_1^+,\perp}$ with the intensities of the transition of the first 2^+ state in the polarization plane $N_{2_1^+,\parallel}$ and perpendicular $N_{2_1^+,\perp}$. The transition widths of electric dipole states resulting from the state-to-state analysis of the DHIPS data and the combination of these with the average branching ratios are visualized in Fig. 4. This parallels the procedure performed in Ref. [47]. In particular for the case of ^{54}Cr, stronger individual excitations as compared to ^{50}Cr and an accumulation of strength are visible in the vicinity of the neutron-separation energy of 9.7 MeV. The fragmentation of this strength resembles those in aforementioned nuclei, in which the PDR has been established.

An examination of the evolution of the transition strength across the neutron shell closure is possible utilizing the Thomas-Reiche-Kuhn (TRK) energy-weighted sum rule [48, 49]. The ratio of the integrated strength assigned to the PDR to the overall strength derived with the TRK sum rule is shown in Fig. 5. The PDR exhausts only about one percent or less of the full strength predicted by the TRK sum rule[1]. Surpassing the shell closure a substantial rise in overall strength is observed.

---

[1] Since the determination of average branching ratios was not possible in the case of ^{52}Cr, branching was accounted for effectively
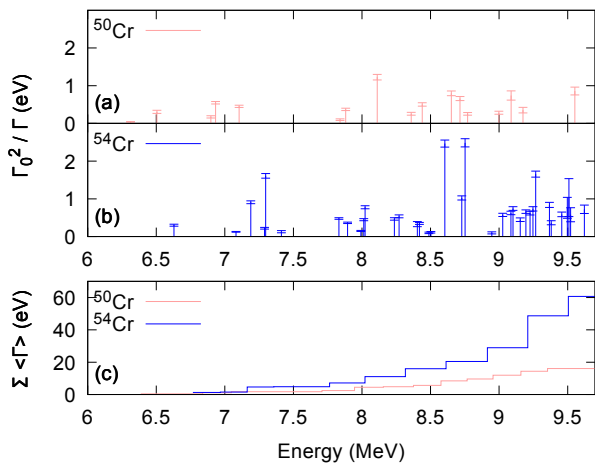
FIG. 4. The transition widths derived from the integrated cross sections of ^{50}Cr and ^{54}Cr measured at DHIPS are shown in panel a) and b), respectively. Only electric dipole transitions are plotted. Running sums of the total transition widths corrected for branching are shown in panel c). Here, the binning corresponds to the beam-energy settings at HIγS.

We note, that no such N-dependent rise is seen in isotopic chains where PDR data measured with one method is available and no major neutron-shell closure is crossed, e.g., the Sn isotopes [50]. This is the first time that such a shell-dependence of the PDR has been studied and observed across a neutron-shell closure. Following the frequently used interpretation of the PDR as a collective excitation, i.e. an oscillation of the neutron skin, a smooth increase is expected as more and more neutrons are added to the nucleus. The behavior of the experimental PDR strength presented in this work, however, leads to the conclusion that the PDR is strongly influenced by the shell structure, as will be discussed below.
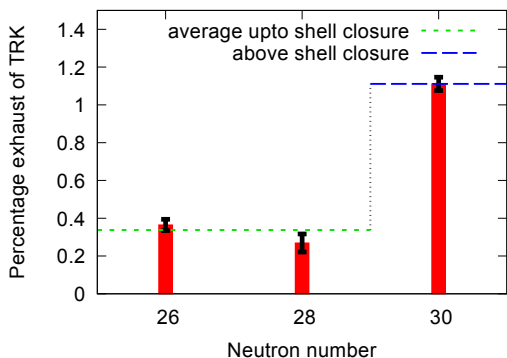
by an additional factor of 1.79. It is equal to the average of the ratios between exhausted percentage with and without branching for both other isotopes. This value's uncertainty of 0.26 is a conservative estimate.

FIG. 5. Behavior of exhausted percentage of the TRK sum rule as a function of neutron number for examined isotopes. A significant increase of the overall strength surpassing the magic neutron number $N = 28$ is evident and highlighted by the horizontal lines. See text for details.

In order to investigate this behavior, the neutron skin thickness of Cr nuclei is calculated using a relativistic mean-field model (RMF) with density-dependent meson-nucleon couplings [51]. It is given by the difference of the root-mean-square radii of neutron and proton density distributions. Nucleons in this model are represented by Dirac spinors that are solutions of the Dirac equation with scalar and vector mean-field potentials. These are obtained self-consistently from scalar (σ) and vector (ω, ρ) meson fields and the electromagnetic potential by solving the corresponding classical field equations with source densities that are determined in turn by the nucleon densities. Corrections for the Coulomb field, the center-of-mass motion, the form factors and radii were included as in [52]. The parametrisation DD2 [53] is used for the density dependence of the couplings, which generates a rearrangement contribution to the vector potential required for consistency. The characteristic empirical nuclear matter parameters of this model, in particular for the symmetry energy at saturation, $J = 31.67$ MeV, and the slope parameter, $L = 55.04$ MeV, are consistent with present constraints from experiment and theory. The results of these calculations for the neutron skin thickness in chromium are shown in Fig. 6.

Similar to the effect seen in the experimental data, adding more weakly-bound neutrons on top of a closed shell does not only lead to a further increase of the low-energy dipole strength, but also enhances abruptly the dependency of the neutron skin thickness ΔR_{np} on the number of neutrons, i.e. a change of the slope of ΔR_{np} with neutron number. Comparable behavior was reported for charge radii in isotopic chains across a neutron shell closures measured in collinear laser spectroscopy [54]. The explanation given in this reference is consistent with our following interpretation: We consider the addition of two neutrons above $N = 28$, which are more loosely bound than those below $N = 28$. Therefore, neutrons added to the core will have a stronger effect on the neutron-skin thickness. In addition, the more loosely-bound neutrons would imply the neutron skin vibration to become softer, i.e. occurring at lower frequency, hence, at lower energy and with a larger amplitude. Such an effect also occurs in model calculations for Sn isotopes [55] and leads to a down-shift of the PDR centroid energy past a shell closure along with an overall increase of the PDR strength. In fact, comparing the running sums of observed $E1$ strength for ^{50,54}Cr in Fig. 4 c), the onset of enhanced strength seems to be shifted about 1 MeV lower in ^{54}Cr.

We conclude, that the onset of the PDR in stable nuclei is observed in the chromium isotopes. Since the two valence-neutrons of ^{54}Cr cause the observed significant increase of $E1$ strength with respect to the isotope ^{50}Cr
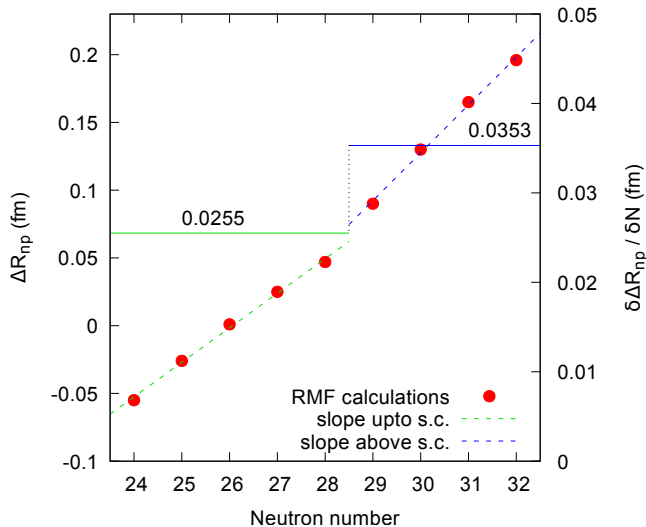
FIG. 6. RMF calculations for chromium isotopes. The calculated neutron skin thicknesses for the isotope chain are shown in red (circles). Two linear fits were added to guide the eye in regards to the behavior for $^{48-52}$Cr upto the shell closure (green/light gray, dashed) and for $^{53-56}$Cr above the shell closure (blue/dark gray, dashed), respectively. The full horizontal lines highlight the slope parameters using the right-hand scale. The overall behavior is also conserved using parametrisations for the density dependency of the symmetry energy of $L = 70$ and $L = 40$ MeV.

with two valence neutron holes, the PDR apparently has its origin in a few-nucleon effect. A statistical analysis [56] had indicated instead, that the PDR states in the stable Cr isotopes might have the properties of a

collective mode. This remains an open question which requires further investigation. The present work shows that correlations between PDR and neutron-skin thickness requires the consideration of shell effects and available valence spaces, especially in the $A \approx 50$ mass region at the emergence of the PDR. We observe, for the first time, a sudden increase of low-lying $E1$ strength across a major shell closure, which is due to the weaker binding of $N > 28$ neutrons. However, to which extent this increase is a result of the faster rate of change of the PDR strength as a function of valence neutrons, or due to the lowering of its centroid energy, needs further exploration in theory and experiment. We emphasize that the calculated change in slope of ΔR_{np} (cf. Fig. 6) is solely due to the structural change and does not necessitate a change of the EOS parameters J and L. This finding should be considered in future attempts to determine the parameters of the EOS from the observable properties of the PDR.

[1] B. P. Abbott, R. Abbott, T. D. Abbott, F. Acernese, K. Ackley, C. Adams, T. Adams, P. Addesso, R. X. Adhikari, V. B. Adya, C. Affeldt, M. Afrough, B. Agarwal, and M. Agathos (LIGO Scientific Collaboration and Virgo Collaboration), Phys. Rev. Lett. **119**, 161101 (2017).

[2] M. Eichler, A. Arcones, A. Kelic, O. Korobkin, K. Langanke, T. Marketin, G. Martinez-Pinedo, I. Panov, T. Rauscher, S. Rosswog, C. Winteler, N. T. Zinner, and F.-K. Thielemann, The Astrophysical Journal **808**, 30 (2015).

[3] F. J. Fattoyev, J. Piekarewicz, and C. J. Horowitz, Phys. Rev. Lett. **120**, 172702 (2018).

[4] A. W. Steiner, J. M. Lattimer, and E. F. Brown, ApJ **722**, 33 (2010).

[5] B.-A. Li, À. Ramos, G. Verde, and I. Vidaña, Eur. Phys. J. A **50**, 9 (2014).

[6] B.-A. Li, L.-W. Chen, and C. M. Ko, Phys. Rep. **464**, 113 (2008).

[7] X. Roca-Maza and N. Paar, Progress in Particle and Nuclear Physics **101**, 96 (2018).

[8] X. Roca-Maza, X. Viñas, M. Centelles, B. K. Agrawal, G. Colò, N. Paar, J. Piekarewicz, and D. Vretenar, Phys. Rev. C **92**, 064304 (2015).

[9] J. Birkhan, M. Miorelli, S. Bacca, S. Bassauer, C. A. Bertulani, G. Hagen, H. Matsubara, P. von Neumann-Cosel, T. Papenbrock, N. Pietralla, V. Y. Ponomarev, A. Richter, A. Schwenk, and A. Tamii, Phys. Rev. Lett. **118**, 252501 (2017).

[10] D. Savran, T. Aumann, and A. Zilges, Progress in Particle and Nuclear Physics **70**, 210 (2013).

[11] W. Bothe and W. Gentner, Zeitschrift für Physik **106**, 236 (1937).

[12] G. C. Baldwin and G. S. Klaiber, Phys. Rev. **71**, 3 (1947).

[13] M. Goldhaber and E. Teller, Phys. Rev. **74**, 1046 (1948).

[14] H. Steinwedel, J. H. D. Jensen, and P. Jensen, Phys. Rev. **79**, 1019 (1950).

[15] A. Bracco, E. Lanza, and A. Tamii, Progress in Particle and Nuclear Physics **106**, 360 (2019).

[16] J. S. Brzosko, E. Gierlik, A. S. Jr., and Z. Wilhelmi, Can J Phys **47**, 2849 (1969).

[17] V. Derya, J. Endres, M. Elvers, M. Harakeh, N. Pietralla, C. Romig, D. Savran, M. Scheck, F. Siebenhühner,

V. Stoica, H. Wörtche, and A. Zilges, Nucl. Phys. A **906**, 94 (2013).

[18] A. Bracco, F. C. L. Crespi, and E. G. Lanza, Eur. Phys. J. A **51**, 99 (2015).

[19] R. Mohan, M. Danos, and L. C. Biedenharn, Phys. Rev. C **3**, 1740 (1971).

[20] J. Piekarewicz, Phys. Rev. C **83**, 034319 (2011).

[21] B. Brown, Phys. Rev. Lett. **85**, 5296 (2000).

[22] U. Kneissl, N. Pietralla, and A. Zilges, J. Phys. G. Nucl. Part. Phys. **32**, R217 (2006).

[23] M. Erhard, A. R. Junghans, C. Nair, R. Schwengner, R. Beyer, J. Klug, K. Kosev, A. Wagner, and E. Grosse, Phys. Rev. C **81**, 034319 (2010).

[24] G. Rusev, R. Schwengner, R. Beyer, M. Erhard, E. Grosse, A. R. Junghans, K. Kosev, C. Nair, K. D. Schilling, A. Wagner, F. Dönau, and S. Frauendorf, Phys. Rev. C **79**, 061302(R) (2009).

[25] C. Romig, J. Beller, J. Glorius, J. Isaak, J. H. Kelley, E. Kwan, N. Pietralla, V. Yu. Ponomarev, A. Sauerwein, D. Savran, M. Scheck, L. Schnorrenberger, K. Sonnabend, A. P. Tonchev, W. Tornow, H. R. Weller, A. Zilges, and M. Zweidinger, Phys. Rev. C **88**, 044331 (2013).

[26] K. Govaert, F. Bauwens, J. Bryssinck, D. De Frenne, E. Jacobs, W. Mondelaers, L. Govor, and V. Yu. Ponomarev, Phys. Rev. C **57**, 2229 (1998).

[27] B. Özel, J. Enders, P. von Neumann-Cosel, I. Poltoratska, A. Richter, D. Savran, S. Volz, and A. Zilges, Nucl. Phys. A **788**, 385 (2007).

[28] R. Schwengner, R. Massarczyk, G. Rusev, N. Tsoneva, D. Bemmerer, R. Beyer, R. Hannaske, A. R. Junghans, J. H. Kelley, E. Kwan, H. Lenske, M. Marta, R. Raut, K. D. Schilling, A. Tonchev, W. Tornow, and A. Wagner, Phys. Rev. C **87**, 024306 (2013).

[29] R. Schwengner, G. Rusev, N. Benouaret, R. Beyer, M. Erhard, E. Grosse, A. R. Junghans, J. Klug, K. Kosev, L. Kostov, C. Nair, N. Nankov, K. D. Schilling, and A. Wagner, Phys. Rev. C **76**, 034321 (2007).

[30] N. Benouaret, R. Schwengner, G. Rusev, F. Dönau, R. Beyer, M. Erhard, E. Grosse, A. R. Junghans, K. Kosev, C. Nair, K. D. Schilling, A. Wagner, and N. Bendjaballah, Phys. Rev. C **79**, 014303 (2009).

[31] R. Schwengner, G. Rusev, N. Tsoneva, N. Benouaret, R. Beyer, M. Erhard, E. Grosse, A. R. Junghans, J. Klug, K. Kosev, H. Lenske, C. Nair, K. D. Schilling, and A. Wagner, Phys. Rev. C **78**, 064314 (2008).

[32] M. Scheck, V. Yu. Ponomarev, T. Aumann, J. Beller, M. Fritzsche, J. Isaak, J. H. Kelley, E. Kwan, N. Pietralla, R. Raut, C. Romig, G. Rusev, D. Savran, K. Sonnabend, A. P. Tonchev, W. Tornow, H. R. Weller, and M. Zweidinger, Phys. Rev. C **87**, 051304(R) (2013).

[33] M. Scheck, V. Yu. Ponomarev, M. Fritzsche, J. Joubert, T. Aumann, J. Beller, J. Isaak, J. H. Kelley, E. Kwan, N. Pietralla, R. Raut, C. Romig, G. Rusev, D. Savran, L. Schorrenberger, K. Sonnabend, A. P. Tonchev, W. Tornow, H. R. Weller, A. Zilges, and M. Zweidinger, Phys. Rev. C **88**, 044304 (2013).

[34] J. Isaak, D. Savran, M. Fritzsche, D. Galaviz, T. Hartmann, S. Kamerdzhiev, J. H. Kelley, E. Kwan, N. Pietralla, C. Romig, G. Rusev, K. Sonnabend, A. P. Tonchev, W. Tornow, and A. Zilges, Phys. Rev. C **83**, 034304 (2011).

[35] T. Hartmann, M. Babilon, S. Kamerdzhiev, E. Litvinova, D. Savran, S. Volz, and A. Zilges, Phys. Rev. Lett. **93**, 192501 (2004).

[36] H. Pai, J. Beller, N. Benouaret, J. Enders, T. Hartmann, O. Karg, P. von Neumann-Cosel, N. Pietralla, V. Yu. Ponomarev, C. Romig, M. Scheck, L. Schnorrenberger, S. Volz, and M. Zweidinger, Phys. Rev. C **88**, 054316 (2013).

[37] J. Wilhelmy, B. A. Brown, P. Erbacher, U. Gayer, J. Isaak, Krishichayan, B. Löher, M. Müscher, H. Pai, N. Pietralla, P. Ries, D. Savran, P. Scholz, M. Spieker, W. Tornow, V. Werner, and A. Zilges, Phys. Rev. C **98**, 034315 (2018).

[38] Krishichayan, M. Bhike, W. Tornow, G. Rusev, A. P. Tonchev, N. Tsoneva, and H. Lenske, Phys. Rev. C **91**, 044328 (2015).

[39] K. Sonnabend, D. Savran, J. Beller, M. Büssing, A. Constantinescu, M. Elvers, J. Endres, M. Fritzsche, J. Glorius, J. Hasper, J. Isaak, B. Löher, S. Müller, N. Pietralla, C. Romig, A. Sauerwein, L. Schnorrenberger, C. Wälzlein, A. Zilges, and M. Zweidinger, Nucl. Instrum. Methods Phys. Res. A **640**, 6 (2011).

[40] N. Pietralla, Nucl. Phys. News **28**, 4 (2018).

[41] H. R. Weller, M. W. Ahmed, H. Gao, W. Tornow, Y. K. Wu, M. Gai, and R. Miskimen, Progress in Particle and Nuclear Physics **62**, 257 (2009).

[42] N. Pietralla, Z. Berant, V. N. Litvinenko, S. Hartman, F. F. Mikhailov, I. V. Pinayev, G. Swift, M. W. Ahmed, J. H. Kelley, S. O. Nelson, R. Prior, K. Sabourov, A. P. Tonchev, and H. R. Weller, Phys. Rev. Lett. **88**, 012502 (2001).

[43] V. N. Litvinenko, B. Burnham, M. Emamian, N. Hower, J. M. J. Madey, P. Morcombe, P. G. O'Shea, S. H. Park, R. Sachtschale, K. D. Straub, G. Swift, P. Wang, Y. Wu, R. S. Canon, C. R. Howell, N. R. Roberson, E. C. Schreiber, M. Spraker, W. Tornow, H. R. Weller, I. V. Pinayev, N. G. Gavrilov, M. G. Fedotov, G. N. Kulipanov, G. Y. Kurkin, S. F. Mikhailov, V. M. Popik, A. N. Skrinsky, N. A. Vinokurov, B. E. Norum, A. Lumpkin, and B. Yang, Phys. Rev. Lett. **78**, 4569 (1997).

[44] See Supplemental Material at [URL will be inserted by publisher] for a table of all examined exited states and thier accessable observables discribed in the work. All files related to a published paper are stored as a single deposit and assigned a Supplemental Material URL. This URL appears in the articles reference list.

[45] D. Savran, M. Elvers, J. Endres, M. Fritzsche, B. Löher, N. Pietralla, V. Y. Ponomarev, C. Romig, L. Schnorrenberger, K. Sonnabend, and A. Zilges, Phys. Rev. C **84**, 024326 (2011).

[46] B. Löher, V. Derya, T. Aumann, J. Beller, N. Cooper, M. Duchêne, J. Endres, E. Fiori, J. Isaak, J. Kelley, M. Knörzer, N. Pietralla, C. Romig, D. Savran, M. Scheck, H. Scheit, J. Silva, A. Tonchev, W. Tornow, H. Weller, V. Werner, and A. Zilges, Nucl. Instrum. Methods Phys. Res. A **723**, 136 (2013).

[47] P. M. Goddard, N. Cooper, V. Werner, G. Rusev, P. D. Stevenson, A. Rios, C. Bernards, A. Chakraborty, B. P. Crider, J. Glorius, R. S. Ilieva, J. H. Kelley, E. Kwan, E. E. Peters, N. Pietralla, R. Raut, C. Romig, D. Savran, L. Schnorrenberger, M. K. Smith, K. Sonnabend, A. P. Tonchev, W. Tornow, and S. W. Yates, Phys. Rev. C **88**, 064308 (2013).

[48] W. Kuhn, Zeitschrift für Physik **33**, 408 (1925).

[49] F. Reiche and W. Thomas, Zeitschrift für Physik **34**, 510 (1925).

[50] H. K. Toft, A. C. Larsen, A. Bürger, M. Guttormsen, A. Görgen, H. T. Nyhus, T. Renstrøm, S. Siem, G. M. Tveten, and A. Voinov, Phys. Rev. C **83**, 044320 (2011).

[51] S. Typel and H. Wolter, Nucl. Phys. A **656**, 331 (1999).

[52] S. Typel, Phys. Rev. C **71**, 064301 (2005).

[53] S. Typel, G. Röpke, T. Klähn, D. Blaschke, and H. H. Wolter, Phys. Rev. C **81**, 015803 (2010).

[54] C. Gorges, L. V. Rodríguez, D. L. Balabanski, M. L. Bissell, K. Blaum, B. Cheal, R. F. Garcia Ruiz, G. Georgiev, W. Gins, H. Heylen, A. Kanellakopoulos, S. Kaufmann, M. Kowalska, V. Lagaki, S. Lechner, B. Maaß, S. Malbrunot-Ettenauer, W. Nazarewicz, R. Neugart, G. Neyens, W. Nörtershäuser, P.-G. Reinhard, S. Sailer, R. Sánchez, S. Schmidt, L. Wehner, C. Wraith, L. Xie, Z. Y. Xu, X. F. Yang, and D. T. Yordanov, Phys. Rev. Lett. **122**, 192502 (2019).

[55] N. Paar, T. Niki, D. Vretenar, and P. Ring, Phys. Lett. B **606**, 288 (2005).

[56] B. Dietz, B. A. Brown, U. Gayer, N. Pietralla, V. Y. Ponomarev, A. Richter, P. C. Ries, and V. Werner, Phys. Rev. C **98**, 054314 (2018).